

RESEARCH ARTICLE

# Serine 26 in the PomB Subunit of the Flagellar Motor Is Essential for Hypermotility of *Vibrio cholerae*

Petra Halang<sup>‡</sup>, Thomas Vorburger<sup>\*</sup>, Julia Steuber<sup>\*</sup>

Institute of Microbiology, University of Hohenheim (Stuttgart), Stuttgart, Germany

<sup>‡</sup> Current address: Clinical Microbiology, Lund University, Malmö, Sweden

<sup>\*</sup> [T.Vorburger@uni-hohenheim.de](mailto:T.Vorburger@uni-hohenheim.de) (TV); [julia.steuber@uni-hohenheim.de](mailto:julia.steuber@uni-hohenheim.de) (JS)



## Abstract

*Vibrio cholerae* is motile by means of its single polar flagellum which is driven by the sodium-motive force. In the motor driving rotation of the flagellar filament, a stator complex consisting of subunits PomA and PomB converts the electrochemical sodium ion gradient into torque. Charged or polar residues within the membrane part of PomB could act as ligands for Na<sup>+</sup>, or stabilize a hydrogen bond network by interacting with water within the putative channel between PomA and PomB. By analyzing a large data set of individual tracks of swimming cells, we show that S26 located within the transmembrane helix of PomB is required to promote very fast swimming of *V. cholerae*. Loss of hypermotility was observed with the S26T variant of PomB at pH 7.0, but fast swimming was restored by decreasing the H<sup>+</sup> concentration of the external medium. Our study identifies S26 as a second important residue besides D23 in the PomB channel. It is proposed that S26, together with D23 located in close proximity, is important to perturb the hydration shell of Na<sup>+</sup> before its passage through a constriction within the stator channel.

## OPEN ACCESS

**Citation:** Halang P, Vorburger T, Steuber J (2015) Serine 26 in the PomB Subunit of the Flagellar Motor Is Essential for Hypermotility of *Vibrio cholerae*. PLoS ONE 10(4): e0123518. doi:10.1371/journal.pone.0123518

**Academic Editor:** Eric Cascales, Centre National de la Recherche Scientifique, Aix-Marseille Université, FRANCE.

**Received:** November 3, 2014

**Accepted:** February 19, 2015

**Published:** April 15, 2015

**Copyright:** © 2015 Halang et al. This is an open access article distributed under the terms of the [Creative Commons Attribution License](https://creativecommons.org/licenses/by/4.0/), which permits unrestricted use, distribution, and reproduction in any medium, provided the original author and source are credited.

**Data Availability Statement:** All relevant data are within the manuscript and its supporting information.

**Funding:** This work was supported by a grant from the Velux Foundation, Kirchgasse 42, "Zum Rothen Adler", 8001 Zurich, Switzerland (to J.S.). The funders had no role in study design, data collection and analysis, decision to publish, or preparation of the manuscript.

**Competing Interests:** The authors have declared that no competing interests exist.

## Introduction

It is essential for bacteria to be able to move, either away from a repellent or towards an attractive environment [1,2]. Motility is achieved via extracellular helical filaments—called flagella, which can be rotated clock- or counterclockwise [3]. The bacterial flagellum consists of three distinct parts: a hollow filament with a length of 15–20 μm composed of flagellin; the hook, which connects the filament to the motor complex; and the membrane embedded motor complex consisting of a rotor and a stator (Fig 1) (reviewed in [4,5]). Typically, the flagellum is driven either by a proton- or a sodium-motive force [6–9], but the mechanism converting ion flux into torque still remains unclear. The stator complex defines the specificity to either protons or sodium ions, with four MotA and two MotB subunits forming a H<sup>+</sup>-dependent MotA<sub>4</sub>MotB<sub>2</sub> stator [10–14], and the homologous PomA and PomB subunits forming a Na<sup>+</sup>-dependent PomA<sub>4</sub>PomB<sub>2</sub> stator [15–19] (Fig 1). Despite considerable effort [20–23], critical amino acid residue(s) conveying H<sup>+</sup> or Na<sup>+</sup> specificity in the stator could not yet be identified,

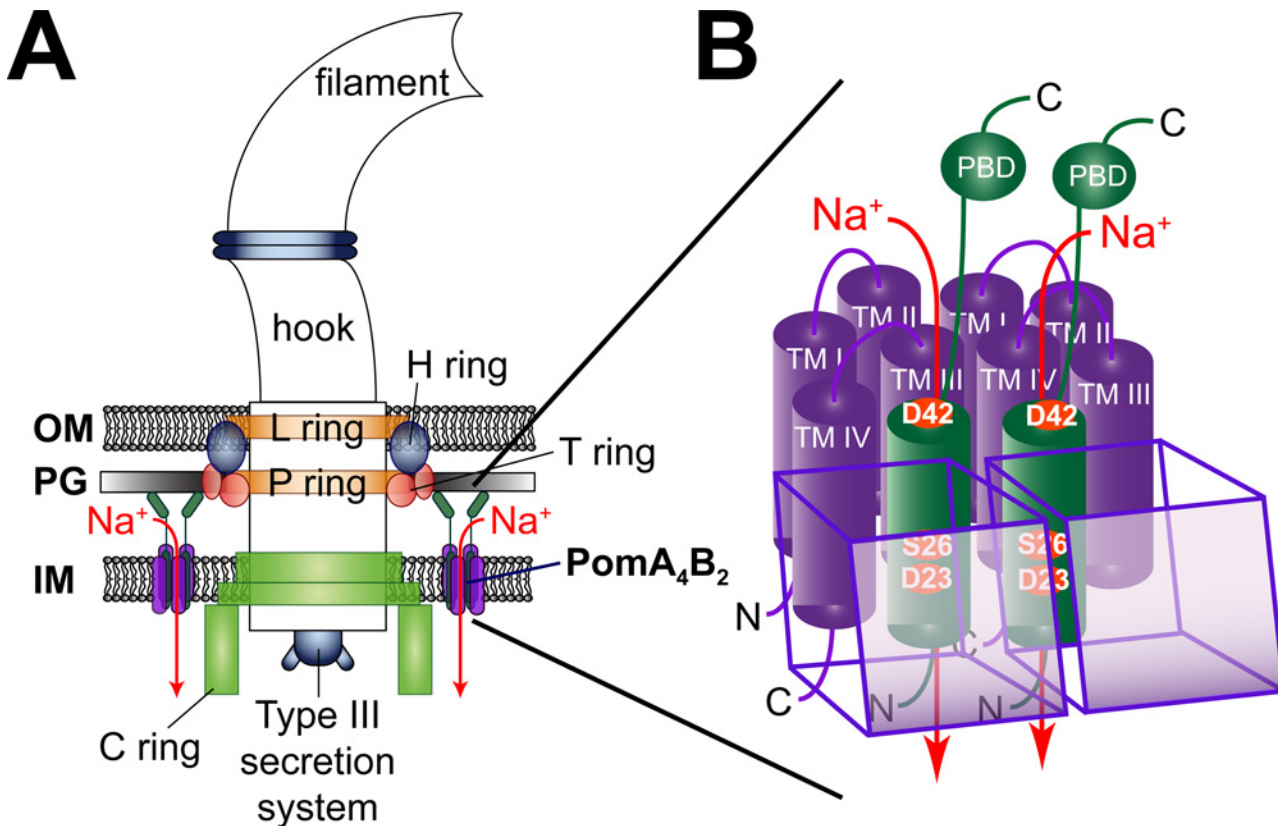


**Fig 1. Rotation of the single polar flagellum from *V. cholerae* is driven by a  $\text{Na}^+$  flux through the  $\text{PomA}_4\text{PomB}_2$  stator complex.** A: The flagellum of *V. cholerae* consists of rotating and static parts. The filament, the hook, which connects the filament to the motor complex, the membrane embedded L and P rings in the outer membrane (OM), and the C ring in the inner membrane (IM) rotate against several stator complexes, each composed of four PomA and two PomB proteins. The H ring functions as a bushing to enable rotation against the peptidoglycan layer (PG). The T ring connects the stator complexes with the peptidoglycan layer. Proton-driven flagella, such as found in *E. coli* and *Salmonella*, do not have H and T rings. Export of protein components of the flagellar filament is catalyzed by a type III secretion system located at the base of the flagellum. B: Four PomA and two PomB subunits form the flagellar stator complex. PomA possesses four transmembrane helices (TM I–IV), PomB only one. The translucent, purple boxes in the front each represent one PomA subunit. The flux of  $\text{Na}^+$  through the stator complex (red arrow) along the chemical gradient drives the rotation of the C ring against the stator elements. It is assumed that  $\text{Na}^+$  ions pass through a channel built by helices III and IV of PomA and the single transmembrane helix of PomB [17,31]. The peptidoglycan binding domain (PBD) in the C-terminal part of PomB stabilizes the stator complexes within the peptidoglycan layer. The conserved amino acid residues D42, S26 and D23 of PomB promote the transport of  $\text{Na}^+$  through the stator [52].

doi:10.1371/journal.pone.0123518.g001

reviewed by Sowa and Berry who stated that “there is no single determining component for ion selectivity” [24]. Most of the bacteria whose flagellar motors were studied to date use a single type of stator complex with a distinct selectivity towards a single coupling ion ( $\text{H}^+$  or  $\text{Na}^+$ ). However, there are exceptions to this rule. One is the metal ion-reducing bacterium *Shewanella oneidensis*. It is motile by means of a single polar flagellum whose motor is, depending on the  $\text{Na}^+$  concentration, equipped with either PomAB ( $\text{Na}^+$ ) or MotAB ( $\text{H}^+$ ) stators [25]. Another exception is the alkaliphilic *Bacillus clausii* that possesses a single, bifunctional stator which couples motility to  $\text{Na}^+$  at the high end of its pH range (pH 7–11), but uses protons at lower pH [26]. Pairs of mutations in *Bacillus clausii* MotB were identified that converted the naturally bifunctional MotAB stator complex into stators that preferentially use either  $\text{H}^+$  or  $\text{Na}^+$  across the full pH range [26]. A dual use of  $\text{Na}^+$  and  $\text{K}^+$  as coupling ions for flagellar motors should also be considered [27].

*V. cholerae* possesses a single, polar flagellum whose  $\text{Na}^+$ -driven motor is equipped with PomAB stator complexes [28,29]. PomA possesses four transmembrane helices and a large

cytoplasmic loop between helix II and III, while PomB consists of one transmembrane helix and a large periplasmic domain (Fig 1) [29]. It was proposed that helices III and IV of the A subunit and the single transmembrane helix of the B subunit are in close proximity to form an ion channel [30–34]. The C terminal part of subunit B—which is essential for stator function—reaches into the periplasmic space and attaches itself to the peptidoglycan layer with its special peptidoglycan binding motif, which increases the stability of the stator complex in the cell membrane [35,36]. The number of stator complexes which surround the motor ranges between 11 and 12 [37,38]. With regard to the high rotational speeds (up to 1700 Hz) which were determined for the sodium-dependent polar flagellum of *V. alginolyticus*, it was first assumed that the rotor and stator complexes of the flagellar motor might form a tight and stable complex [39]. Nonetheless it could be demonstrated that stator complexes dynamically associate with or dissociate from the motor without disrupting flagellar rotation [37], in equilibrium with a pool of membrane embedded, inactive stator complexes [40,41]. It is assumed that upon ion influx, conformational changes occur in the cytoplasmic loop of PomA bringing the cytoplasmic loop in close proximity to FliG [42]. Charged residues of this cytoplasmic loop interact with charged residues residing in the C-terminal domain of FliG. FliG is part of the torque generating machinery and switch complex responsible for changing the direction of flagellar motor rotation. It also participates in the assembly of the flagellum and is important for efficient stator assembly around a rotor [22,43–51]. When searching for a putative ion pathway through the flagellar motor, one has to consider the topology and the position of charged amino acid residues in the membrane-embedded stretches of the stator. We recently showed that D23, S26, and D42 of PomB are part of ion-conducting pathway(s) in the PomA<sub>4</sub>B<sub>2</sub> stator complex of the Na<sup>+</sup>-driven flagellum from *V. cholerae* [52]. In the present study, a large number of tracks of *V. cholerae*  $\Delta pomAB$  cells expressing PomB-S26A or PomB-S26T variants were analyzed to study the influence of pH and salt on the distribution of swimming speeds. To this end, a novel microscopic approach was applied which did not require staining of cells with fluorophores. It has been suggested that the exchange of PomB-S26 (conserved in Na<sup>+</sup>-dependent flagellar motors) for a conserved threonine at the corresponding position in H<sup>+</sup>-dependent motors might reflect their different ion specificity [53]. Here we show that S26 is critical to promote very fast rotation of the flagellum of *V. cholerae*. We propose that S26 is important for the orientation of water molecules, and helps to perturb the hydration shell of Na<sup>+</sup> before entering the selectivity filter of the channel in the stator.

## Materials and Methods

### Chemicals, bacterial strains and plasmids

Unless stated otherwise, chemicals were purchased from Sigma-Aldrich Chemie GmbH, Germany. Yeast extract, tryptone, and bacto agar were purchased from Becton, Dickinson. The *V. cholerae* strains used in this study were O395-N1 [54], O395-N1  $\Delta pomAB$  ( $\Delta ctxA$  Str<sup>r</sup>  $\Delta pomAB$ ) [22] and O395-N1  $\Delta nqr$  ( $\Delta ctxA$  Str<sup>r</sup>  $\Delta nqrA-F$ ) [55]. The plasmids used in this study are listed in Table 1.

**Table 1. Plasmids used in this study.**

Plasmid	Relevant characteristics	Reference
pAB	<i>P<sub>araBAD</sub></i> , codes for His <sub>6</sub> -PomA and PomB-Strep, Ap <sup>r</sup>	[29,52]
pAB-S26A	<i>P<sub>araBAD</sub></i> , codes for His <sub>6</sub> -PomA and S26A variant of PomB-Strep, Ap <sup>r</sup>	[52]
pAB-S26T	<i>P<sub>araBAD</sub></i> , codes for His <sub>6</sub> -PomA and S26T variant of PomB-Strep, Ap <sup>r</sup>	[52]
pISC-H	Empty vector of pAB	[29]

doi:10.1371/journal.pone.0123518.t001

## Isolation of total RNA from *V. cholerae*

5 ml LB-Na<sup>+</sup> (1% tryptone, 0.5% yeast extract, 171 mM NaCl, 50 μg ml<sup>-1</sup> streptomycin, pH 7.0) was inoculated with an overnight culture of either *V. cholerae* reference strain or *V. cholerae* Δ*pomAB* transformed with pAB to an OD<sub>600</sub> of 0.01. Ampicillin (200 μg ml<sup>-1</sup>) and L-(+)-arabinose (10 mM) was added for *V. cholerae* Δ*pomAB* pAB. Cells were grown aerobically at 30°C / 180 rpm (orbit: 25 mm) until an OD<sub>600</sub> of approximately 0.5 was reached, harvested by centrifugation (2 min, 11,000 rpm) and washed in 1 ml RNAlater (Qiagen). Cells were harvested (2 min, 11,000 rpm) and resuspended in 0.5 ml TE buffer (30 mM Tris-HCl, 1 mM EDTA, pH 8.0) containing lysozyme (5 mg ml<sup>-1</sup>), CaCl<sub>2</sub> (1 mM), MgCl<sub>2</sub> (1 mM) and DNase I (a few crystals were dissolved in 10 ml of TE buffer). Cells were incubated at 30°C for 20 min prior to addition of proteinase K (1 mg ml<sup>-1</sup>). Incubation at 30°C was continued (15 min), and RNA was purified using the RNeasy Mini Kit (Qiagen) according to the manufacturer's protocol. The quality of the isolated RNA was assessed by gel electrophoresis. RiboRuler High Range RNA Ladder (Thermo Scientific) was used as molecular standard. We did not detect bands beside the 23S and 16S rRNA, indicating the absence of genomic DNA. The RNA yield was 414 ng μl<sup>-1</sup> from the *V. cholerae* reference strain and 130 ng μl<sup>-1</sup> from the *pomAB* deletion strain transformed with pAB.

## Real-Time Quantitative Reverse Transcription PCR (qRT-PCR)

The SuperScript III First-Strand Synthesis System for RT-PCR (Invitrogen) was used for the synthesis of cDNA according to the manufacturer's protocol using random hexamer primers. The yields of the cDNA preparations that served as template source for the qRT-PCR reactions were 166 ng μl<sup>-1</sup> for the *V. cholerae* reference strain and 52 ng μl<sup>-1</sup> for *V. cholerae* Δ*pomAB* pAB. The SensiFAST SYBR & Fluorescein Kit (Bioline) was used to determine the expression level of *pomB* in qRT-PCR reactions using primer pairs "pomB fwd" (5'-CGCAGTTTCG GTGGCGCAAG-3') and "pomB rev" (5'-TGCCCGTTGCGCTTCGGTAT-3'). A reaction mix (20 μl) contained 20 pmol of each primer and 100 ng cDNA. qRT-PCR reactions were performed in triplicates using a CFX96 cycler (Bio-Rad) with following cycling conditions: 1.95°C for 2 min, 2.95°C for 10 s, 3.60°C for 20 s, 4.95°C for 10 s, and a final melting curve with a temperature range from 65°C to 95°C (0.5°C increment). Steps 2 and 3 were repeated 39 times. The correct size (134 bp) of the qRT-PCR products was confirmed by gel-electrophoresis using a 100 bp DNA ladder (GeneRuler, Thermo Scientific). Primer efficiencies (with 100 ng, 10 ng, 1 ng, 0.1 ng cDNA as template) and relative gene expression of *pomB* from the *V. cholerae* reference strain and *V. cholerae* Δ*pomAB* pAB were quantified using the CFX Manager software (Bio-Rad, version 2.1.1022.0523). The primer efficiency was 115% with R<sup>2</sup> = 0.998.

## Detection of PomB variants on Western blots

5 ml LB-Na<sup>+</sup> (1% tryptone, 0.5% yeast extract, 171 mM NaCl, 10 mM Tris base, 50 μg ml<sup>-1</sup> streptomycin, 200 μg ml<sup>-1</sup> ampicillin, pH adjusted to 8.0 with 5 M KOH) was inoculated to an OD<sub>600</sub> of 0.01 with an overnight culture of *V. cholerae* Δ*pomAB* transformed with pISC-H, pAB, pAB-S26A or pAB-S26T, respectively. Overexpression of His<sub>6</sub>-PomA together with PomB-Strep (wild type), PomB-S26A-Strep or PomB-S26T-Strep was performed in the presence of 10 mM L-(+)-arabinose. After 4 h of growth at 30°C / 180 rpm (orbit: 25 mm), cells were harvested by centrifugation (15 min, 11,000 rpm) and resuspended in SDS loading buffer to a final OD<sub>600</sub> of 5.0. Assuming that 1 U of absorbance at 600 nm corresponds to 0.33 g total dry weight per liter [56] and that 55% of the total dry weight represents protein [57], the 20 μl of the cell suspension in SDS loading buffer which were loaded onto the SDS-PAGE gel per lane contained 18 μg total protein. SDS-PAGE and Western blot analysis were performed as described in [29].

## Motility of *V. cholerae* on softagar plates

Motility assays were performed on LB softagar plates pH 8.0 as described in [58] with the following L-(+)-arabinose concentrations: 0, 0.001, 0.01, 0.1, 1.0, 10 and 20 mM. Plates were incubated at 30°C for 21 h. The average and standard deviations were calculated with eight experiments from a total of 10 experiments (the lowest and highest values were omitted).

## Determination of swimming speeds by microscopy

With *V. cholerae*, we did not observe any motile cells in the buffer used by Homma and co-workers to study motility of *V. alginolyticus* [53]. Instead, experiments were performed in LB-based tracking media (1% tryptone, 0.5% yeast extract, 10 mM Tris base, 50  $\mu\text{g ml}^{-1}$  streptomycin) without added salts, or with 171 mM NaCl (LB-Na<sup>+</sup>) or 171 mM KCl (LB-K<sup>+</sup>). The pH was adjusted to 7.0, 8.0 or 9.0 with 5 M HCl or 5 M KOH. Media for *V. cholerae*  $\Delta\text{pomAB}$  transformed with plasmids pAB, pAB-S26A or pAB-S26T contained 200  $\mu\text{g ml}^{-1}$  ampicillin and 10 mM L-(+)-arabinose. The residual Na<sup>+</sup> and K<sup>+</sup> concentrations in the medium without added salts were 11 mM and 12 mM, as determined by atomic absorption spectroscopy (Shimadzu AA-6200). An overnight culture of a given *V. cholerae* strain grown in LB-Na<sup>+</sup> at 37°C was diluted in LB-based tracking medium with indicated pH and salt content to an OD<sub>600</sub> of 0.01. Cells were incubated at 30°C under shaking (180 rpm, orbit: 25 mm) for 4 h in media with salt added, or 5 h in media without added salts. Cells were diluted 1:100 in the same medium, and 50 mM L-serine was added to enhance straight swimming of the bacteria. An aliquot (30  $\mu\text{L}$ ) was pipetted into one channel of a flat  $\mu$ -Slide VI (Ibidi, Germany), and cells were immediately observed under 200-fold magnification using an upright fluorescence microscope (Imager M1, Zeiss, Germany) in its differential interference contrast (DIC) mode. The microscope was equipped with a standard CCD camera (AxioCam MRm, Zeiss, Germany) and controlled using the software AxioVision (Zeiss, Germany; release 4.7) including a real-time video recorder function (Fast Acquisition Module, Zeiss, Germany). After determination of adequate settings for the light exposure using the auto-exposure function of AxioVision and manual focusing in the z-axis to the middle between the base and the top of the channel, about 30 series of time sequences were taken. The typical exposure time was 20 ms, and the constant interval between two consecutive images was 50 ms. The total length of a typical sequence of images was 12 s, corresponding to 250 individual images in one tracking experiment. At least 305 tracks per condition and strain were recorded and analyzed by the WimTaxis software (Wimasis GmbH, Germany). All bacterial cells showing a minimum speed of 4  $\mu\text{m s}^{-1}$  were included in the analysis. Bacterial cells were divided into three main classes according to their measured swimming speeds, namely class I: from 4  $\mu\text{m s}^{-1}$  to less than 18  $\mu\text{m s}^{-1}$  (“slow swimmers”), class II: from 18  $\mu\text{m s}^{-1}$  to less than 41  $\mu\text{m s}^{-1}$  (“medium swimmers”), and class III: 41  $\mu\text{m s}^{-1}$  and faster (“fast swimmers”). Results were presented in histograms created with the help of the software Origin (release 8.0). The average of velocities in a given class, the standard deviation, the mean and the median were calculated using Origin.

## Membrane potential ( $\Delta\psi$ ) measurements

$\Delta\psi$  established by *V. cholerae* cells was assayed using the BacLight Bacterial Membrane Potential Kit (Invitrogen) basically according to the manufacturer's instructions. The staining dye 3,3'-diethyloxycarbocyanine iodide (DiOC<sub>2</sub>) exhibits green fluorescence, but self-associates when entering the cells, resulting in a shift towards red fluorescence. The uptake of DiOC<sub>2</sub> is promoted by  $\Delta\psi$  (inside negative), thus cells with higher  $\Delta\psi$  exhibit increased red fluorescence. *V. cholerae*  $\Delta\text{pomAB}$  transformed with pAB, pAB-S26A or pAB-S26T, as well as *V. cholerae*  $\Delta\text{nqr}$ , were streaked onto LB agar plates with appropriate antibiotics and cultivated over night



at 37°C. 5 ml of LB medium with indicated salt composition and pH containing the appropriate antibiotics was inoculated with a single colony of each strain and incubated overnight at 37°C / 180 rpm (orbit: 25 mm). 3 ml LB-Na<sup>+</sup> or LB-K<sup>+</sup> were inoculated with the overnight culture to an OD<sub>600</sub> of 0.01 and incubated at 30°C / 180 rpm (orbit: 25 mm) for 4 h. Expression of His<sub>6</sub>-PomA and PomB-Strep (wild type or S26A and S26T variants) was started immediately by adding L-(+)-arabinose (final concentration: 10 mM). When LB medium without added salt was used, cultures were incubated at 30°C / 180 rpm for 5 h. The final OD<sub>600</sub> of each culture was determined and the cultures were diluted in phosphate buffered saline (PBS; 10 mM Na-phosphate, 145 mM NaCl, pH 7.4) to a final OD<sub>600</sub> of 0.1. Cells were washed in 1 ml PBS, sedimented by centrifugation (16,000 rpm, 15 min) and resuspended in 1 ml PBS. 5 μl DiOC<sub>2</sub> (final concentration: 15 μM) was added to the cell suspensions from a 3 mM stock solution in DMSO. Cell-free buffer controls contained PBS with or without DiOC<sub>2</sub>. The cells were incubated at room temperature for 1 h. Subsequently, aliquots of 200 μl were transferred into a black, 96 well plate (4ti-0263, 4titude) to determine red (635 nm, band width 35 nm, gain: 49–53) fluorescence emission intensities using a TECAN Infinite F200 PRO plate reader. The excitation wavelength was 485 nm with a band width of 20 nm. After the measurements, the samples were transferred into a translucent, 96 well plate (4ti-0224, 4titude) and the OD<sub>595</sub> was determined using the plate reader. Statistical analyses were performed using Origin (release 8.0). For each strain and condition, three biological and three technical replicates were performed. The fluorescence intensity of PBS without cells but with dye (background) was subtracted from the fluorescence intensities of the stained cell suspensions.

## Results

### Overproduction of PomA<sub>4</sub>B<sub>2</sub> stator complexes and its variants in *V. cholerae* Δ*pomAB*

To estimate the level of overexpression of *pomB*, we performed qRT-PCR on *pomB*, using cDNA produced from total RNA of *V. cholerae* Δ*pomAB* transformed with plasmid pAB (Table 1). In the presence of 10 mM L-arabinose, the transcript levels were drastically increased (110-fold) in *V. cholerae* Δ*pomAB* transformed with pAB compared to the reference strain containing chromosomally encoded *pomAB* (Fig 2). This overexpression of *pomB* (together with *pomA*) from plasmid pAB is in accord with the previously observed accumulation of GFP-tagged stators at cell poles and at the inner membrane, using a plasmid derived from pAB in the same *V. cholerae* host, and with identical inducer concentration [52]. The strong expression of His<sub>6</sub>-PomA and PomB-Strep from plasmid pAB and its derivatives is also in accordance with our previous observation that production of PomB-Strep-D23N in the *V. cholerae* reference strain containing chromosomally encoded *pomB* resulted in drastically reduced motility compared to the reference strain transformed with the empty vector. PomB-D23N-Strep is an inactive variant of PomB-Strep which, together with His-tagged PomA, was inserted into the polar flagellum, replacing the endogenous, active PomA<sub>4</sub>PomB<sub>2</sub> stators [29]. Likewise, introducing the D23E or D23N mutations did not alter the amount of overproduced PomB-Strep variant when compared to wild type PomB-Strep, as estimated from the intensity of PomB-Strep detected with Strep-Tactin-horseradish peroxidase conjugate on Western blots [29]. The present study showed that replacing S26 in PomB-Strep with A or T did not result in decreased expression when compared to wild type PomB-Strep (Fig 3). In accord with the Western blot analysis, similar high levels of mRNA of the mutated variants were assumed. Previously, GFP-tagged variants of PomB carrying the S26A and S26T mutations and wild type GFP-PomB were shown to exhibit similar expression levels and localization at the inner membrane [52]. The calculated molecular mass of PomB-Strep is 36.7 kDa, but the protein runs at an apparent

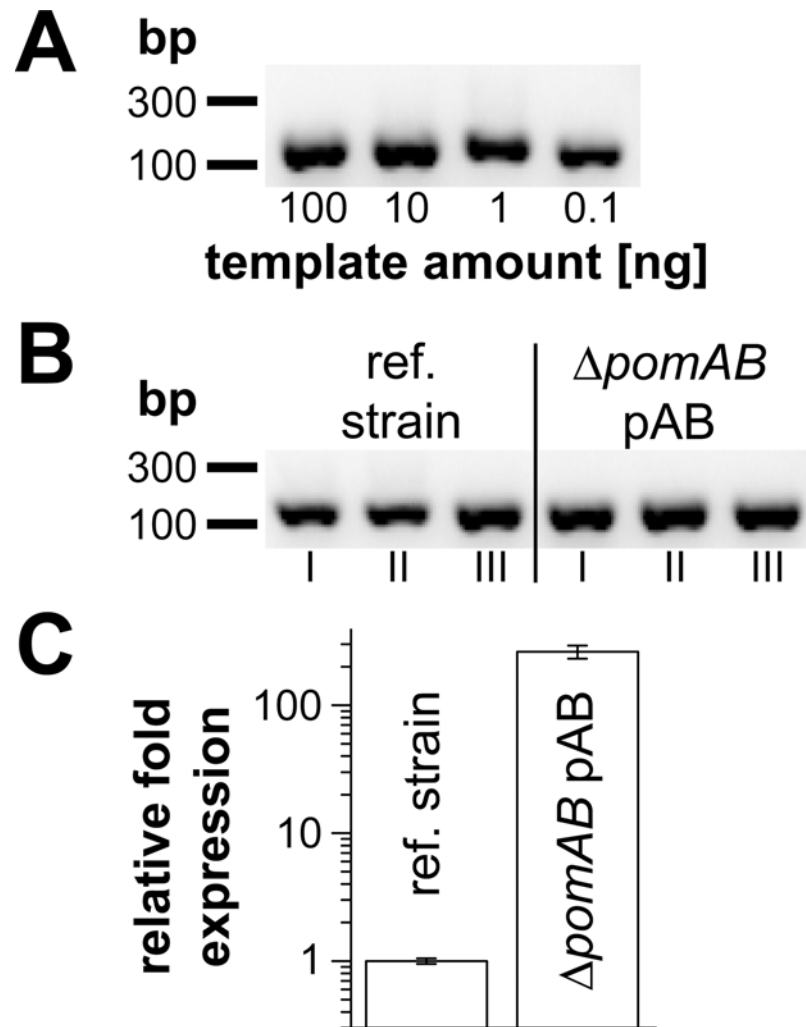


**Fig 2. Transcription level of plasmid-encoded versus chromosomally encoded *pomB* in *V. cholerae* determined by qRT-PCR.** A: analysis of amplification products obtained from qRT-PCR reactions with template (cDNA) amounts of 100 ng, 10 ng, 1 ng and 0.1 ng by agarose gel electrophoresis. The efficiency of the primer pair “*pomB fwd*” / “*pomB rev*” was 115% with  $R^2 = 0.998$ , as calculated using the CFX Manager software (Bio-Rad). A 100 bp DNA ladder (GeneRuler, Thermo Scientific) served as molecular size marker. B: The correct size (134 bp) of the products from the qRT-PCR reactions (technical triplicates, I–III) was confirmed by agarose gel electrophoresis. C: Relative transcription level of *pomB* in the *V. cholerae* reference strain and in *V. cholerae*  $\Delta pomAB$  pAB induced with 10 mM L-arabinose. For both strains, qRT-PCR reactions were performed in technical triplicates. Transcription levels of *pomB* were calculated using the CFX Manager software (Bio-Rad, version 2.1.1022.0523), and the transcription level of the chromosomally encoded *pomB* (reference strain) was set to 1.

doi:10.1371/journal.pone.0123518.g002

molecular mass of almost 46 kDa on SDS-PAGE. In the absence of L-arabinose, *V. cholerae* did not produce PomB-Strep at detectable levels. The band at a molecular weight around 70 kDa represents a biotinylated protein from *V. cholerae* found in all strains in the absence or presence of inducer. Considering this strong overproduction of stator complexes in the presence of 10 mM L-arabinose, confirmed for PomB-Strep here on the level of mRNA, and previously on the level of protein [52], we conclude that overall motility of cells was not limited by the availability of pre-assembled stator complexes [58,59]. This was further confirmed in experiments designed to identify the concentration range of the inducer L-arabinose required for maximum

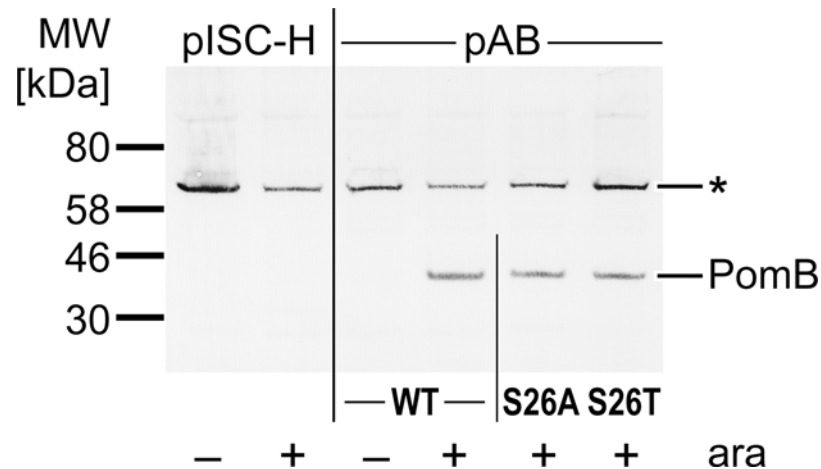


**Fig 3. Expression levels of plasmid-encoded PomB variants in *V. cholerae*  $\Delta pomAB$ .** Wild type PomB-Strep, PomB-S26A-Strep and PomB-S26T-Strep were detected in extracts from *V. cholerae*  $\Delta pomAB$  cells transformed with variants of plasmid pAB on a Western blot. PomB-Strep with an apparent molecular weight around 46 kDa was expressed in the presence (+) but not in the absence (-) of 10 mM L-arabinose, and it was also absent in extracts from *V. cholerae*  $\Delta pomAB$  transformed with the empty vector (pISC-H). Cells were grown for 4 h at 30°C, harvested and resuspended in SDS loading buffer to a final OD<sub>600</sub> of 5.0. Per lane, an aliquot of 18  $\mu$ g total cell protein was loaded. The bands (\*) above the 58 kDa marker result from detection of an endogenous, biotinylated protein of *V. cholerae* by the Strep-Tactin-horseradish peroxidase conjugate [52].

doi:10.1371/journal.pone.0123518.g003

motility on softagar plates (Fig 4). Motility was followed on LB-Na<sup>+</sup> softagar plates at pH 8.0. When the L-arabinose concentration was raised from 0.01 to 0.1 mM, there was a steep increase in motility of *V. cholerae*  $\Delta pomAB$  transformed with plasmids coding for His<sub>6</sub>-PomA together with wild type PomB-Strep, PomB-S26A-Strep or PomB-S26T-Strep (Fig 4). The largest motility rings were observed in the range from 1 to 10 mM L-arabinose. A further increase to 20 mM L-arabinose led to a decrease of motility in all strains. To study the effect of S26 mutations in PomB on motility of *V. cholerae*, tracking experiments were performed in the presence of 10 mM L-arabinose, as described in the following section.

### Tracking live *V. cholerae* cells by differential interference contrast microscopy

An important prerequisite for the tracking of swimming cells by light microscopy is a clear contrast between the individual cells and their surrounding space. In a previous study, we described the use of a fluorescent dye (MitoTracker, Invitrogen) to visualize *V. cholerae* cells by their fluorescence signal upon excitation with light of a distinct wavelength [29]. The advantage of this method is that it produces images of single cells which, at 200-fold magnification, appear as bright, point-shaped objects in front of a dark background. Such objects cannot only be safely detected by spot detection algorithms, they can also be tracked quite easily by tracking algorithms provided by commercially available image processing software like Volocity (Perkin Elmer, USA) or Imaris (Bitplane AG, Switzerland). However, there are disadvantages. One is that in the presence of the fluorescent dye, we observed a large fraction of immotile cells which produce significantly stronger fluorescent signals than motile cells do, and that these stronger signals tend to overlay the weaker signals of swimming cells, especially those of fast swimming cells. This particularly becomes a problem when a small fraction of fast swimming cells is to be analyzed in the presence of a considerable number of non-swimming cells. Another disadvantage is that the fluorescence signal from MitoTracker stained cells bleaches out quite rapidly,



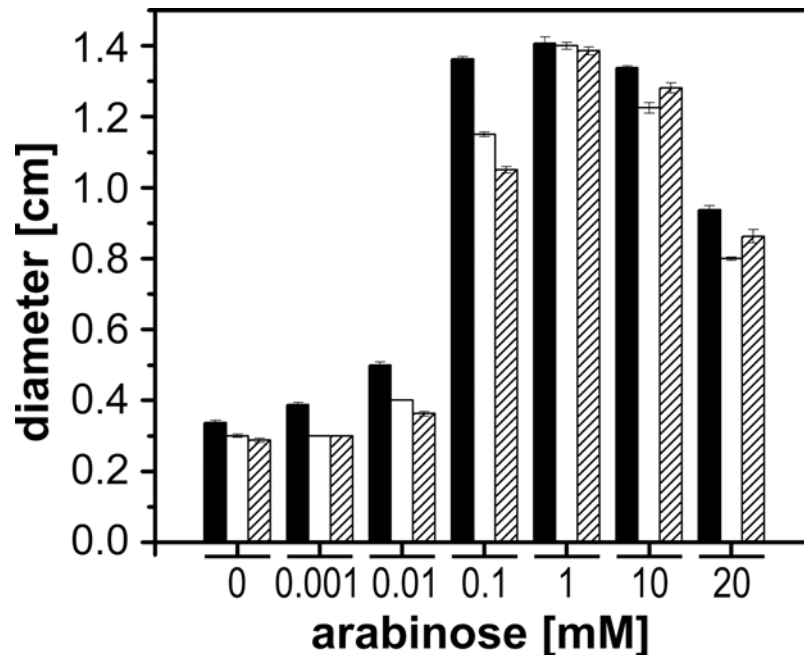


**Fig 4. Influence of inducer concentration on motility of *V. cholerae*  $\Delta pomAB$  overproducing His<sub>6</sub>-PomA together with PomB-Strep, PomB-S26A-Strep, or PomB-S26T-Strep.** The average and standard deviations were calculated of eight experiments (the lowest and highest values from a total of ten experiments were omitted). Black bars: *V. cholerae*  $\Delta pomAB$  pAB; open bars: *V. cholerae*  $\Delta pomAB$  pAB-S26A; hatched bars: *V. cholerae*  $\Delta pomAB$  pAB-S26T.

doi:10.1371/journal.pone.0123518.g004

preventing the recording of video sequences over longer periods of time. The method described here allows determination of velocities of a large number of cells in the absence of fluorescent dyes, i.e. under physiological conditions. The majority of cells (>90%) is motile under all conditions tested here. Tracking of cells is not impaired by bleaching of the fluorophore, and there is no background fluorescence caused by immotile cells which could interfere with the automated tracking of motile cells.

### Overproduction of PomA and PomB promotes fast swimming of *V. cholerae*

There is a continuous replacement of stators in the flagellum using pre-assembled PomA<sub>4</sub>B<sub>2</sub> complexes [37,59]. With a vector system for low expression of PomA and PomB, a limitation in stator complexes could decrease motility compared to the reference strain with endogenous *pomA* and *pomB* genes. On the other hand, a vector allowing for high expression could result in an overload of pre-assembled stator complexes, possibly interfering with the insertion of the stators, and impairing flagellar function. Using a low-expression vector for the production of stator complexes, Berry and coworkers [58] observed a distribution of rotation speeds using beads attached to a single, truncated flagellar filament of an *E. coli* cell fixed to a glass surface. The rotational speeds were presented in histograms, and the authors assumed that the distinct frequencies resulted from different numbers of stator units present in the flagellar motor of the cell. In that study which was performed with a chimeric, Na<sup>+</sup>-dependent stator, the slowest major peak in each histogram was assigned to the frequency of a flagellar motor containing a single stator unit [58]. In our previous studies [29,52], we found no evidence for an inhibition

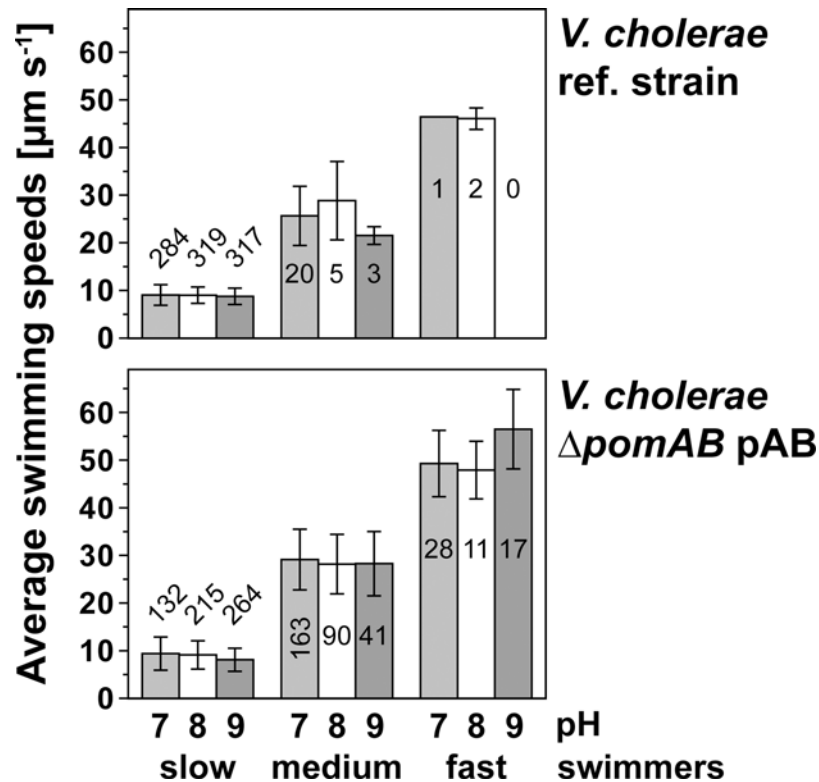


**Fig 5. Distribution of swimming speeds of the *V. cholerae* reference strain and of *V. cholerae*  $\Delta pomAB$  expressing *pomA* and *pomB* in trans.** Tracks were recorded in LB-Na<sup>+</sup> adjusted with Tris to pH 7.0 (light grey bars), pH 8.0 (white bars), or pH 9.0 (dark grey bars). Tracking results of individual cells were assigned to three main classes of velocities (“slow”, “medium” and “fast”). The numbers in the bars indicate the number of tracks used to calculate the mean values and standard deviations. Minimum, median and maximum values are given in the supporting information (S1 Table).

doi:10.1371/journal.pone.0123518.g005

of motility of *V. cholerae*  $\Delta pomAB$  overexpressing its endogenous, Na<sup>+</sup>-dependent stator complexes at an inducer concentration of 10 mM L-arabinose, a finding which is further substantiated in motility experiments on soft agar plates (Fig 4). The fastest swimmers among these cells were expected to operate flagellar motors with maximum occupancy of stator complexes. We tested if overproduction of the PomA<sub>4</sub>PomB<sub>2</sub> stator in *V. cholerae*  $\Delta pomAB$  had an effect on the swimming speed of individual cells when compared to the reference strain. Irrespective of the strain and the pH (7.0, 8.0, or 9.0) of the medium studied, *V. cholerae* cells exhibited large variations in swimming speeds. For better comparison of the results, velocity classes from 4 to <18  $\mu\text{m s}^{-1}$  (slow swimmers), 18 to <41  $\mu\text{m s}^{-1}$  (medium swimmers), or 41  $\mu\text{m s}^{-1}$  and faster (fast swimmers) were defined (Fig 5). In Fig 5, the numbers in the bars represent the number of tracks analyzed to obtain the mean velocity and standard deviation of the given class. We also determined the median of velocities of a given class, yielding a similar result with respect to interpretation of the data (S1 Table). In LB-Na<sup>+</sup> medium, the majority of the analyzed cells of the *V. cholerae* reference strain (wild type) exhibited slow swimming speeds between 4  $\mu\text{m s}^{-1}$  and <18  $\mu\text{m s}^{-1}$  at all proton concentrations of the medium tested (Fig 5). In LB-Na<sup>+</sup>, the greatest speed determined for the *V. cholerae* reference strain (48  $\mu\text{m s}^{-1}$ ) was observed in medium buffered to pH 8.0 (S1 Table). However, only a small subset of cells exhibited high velocities at pH 7.0 and 8.0, while the majority fell into the medium and, first of all, into the slow swimmer classes. When the pH was raised to 9.0, we did not observe any cells faster than

23  $\mu\text{m s}^{-1}$  (S1 Table). Interestingly, a different distribution of swimming speeds was observed with the *V. cholerae*  $\Delta pomAB$  strain expressing plasmid-encoded wild type His<sub>6</sub>-PomA and PomB-Strep, containing increased amounts of PomA<sub>4</sub>PomB<sub>2</sub> stator complexes (Fig 5). At all pH values tested (7.0, 8.0 and 9.0), the *V. cholerae*  $\Delta pomAB$  strain, transformed with plasmid pAB encoding for His-tagged *pomA* and Strep-tagged *pomB*, exhibited higher motilities than the reference strain. This is most obvious when comparing either the distribution of cells over the three main classes of swimming speeds, or their top speeds. Particularly, the medium (18  $\mu\text{m s}^{-1}$  to <41  $\mu\text{m s}^{-1}$ ) as well as the fast (41  $\mu\text{m s}^{-1}$  or faster) speed classes were much more populated by the complemented *pomAB* deletion strain than by the reference strain (Fig 5). Whereas top swimming speeds of up to 61  $\mu\text{m s}^{-1}$  (LB-Na<sup>+</sup> pH 8.0), 73  $\mu\text{m s}^{-1}$  (LB-Na<sup>+</sup> pH 9.0) or even 74  $\mu\text{m s}^{-1}$  (LB-Na<sup>+</sup> pH 7.0) were observed with complemented  $\Delta pomAB$  cells, the fastest cells of the reference strain were slower (48  $\mu\text{m s}^{-1}$  at pH 8.0, 40  $\mu\text{m s}^{-1}$  at pH 7.0), especially at pH 9.0 (23  $\mu\text{m s}^{-1}$ ) (S1 Table). It is noteworthy that the highest speed (94  $\mu\text{m s}^{-1}$ ) of *V. cholerae*  $\Delta pomAB$  transformed with plasmid pAB was observed in LB-K<sup>+</sup> (pH 8.0) (Fig 6, and S2–S4 Tables), but not in LB-Na<sup>+</sup>. In summary, the endogenous levels of PomA and PomB

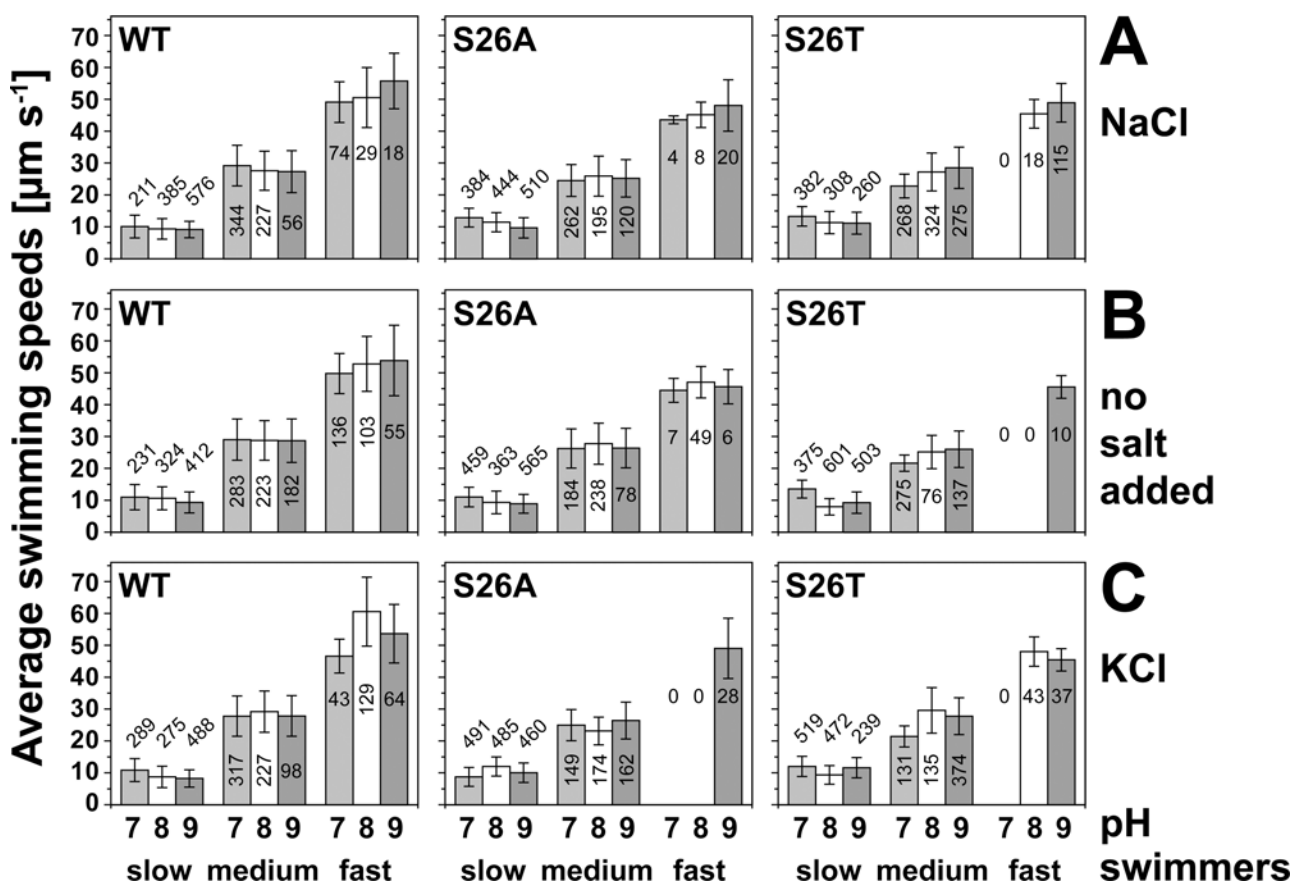


**Fig 6. Influence of pH and salt condition on the swimming speeds of *V. cholerae*  $\Delta pomAB$  cells overproducing His<sub>6</sub>-PomA together with PomB-Strep, PomB-S26A-Strep, or PomB-S26T-Strep.** Tracks were recorded in different LB media adjusted with Tris to pH 7.0 (light grey bars), pH 8.0 (white bars), or pH 9.0 (dark grey bars). A: LB-Na<sup>+</sup>; B: no salt added, with residual concentrations of 11 mM Na<sup>+</sup> and 12 mM K<sup>+</sup>; C: LB-K<sup>+</sup>. Tracking results of individual cells were assigned to three main classes of velocities (“slow”, “medium” and “fast”). The numbers in the bars represent the number of tracks recorded under the specified condition. The mean values and standard deviations of velocities are presented. Minimum, median and maximum values are given in the supporting information (S2–S4 Tables).

doi:10.1371/journal.pone.0123518.g006

in the *V. cholerae* reference strain were insufficient to promote maximum velocity, at least under the chosen conditions (LB medium with Tris buffer). Therefore, overexpression from plasmid pAB was a prerequisite to study the effect of mutations within the Na<sup>+</sup> channels on fast swimming, as described in the following section.

### S26 in PomB is critical for fast swimming of *V. cholerae* cells

We previously showed that motility of *V. cholerae* cells critically depends on osmolality and pH [52]. The analysis of a large set of cell tracks, followed by assignment to distinct classes of velocities, revealed an unexpected phenotype of cells carrying mutations at position S26 of PomB from *V. cholerae*. We recorded at least 631 tracks per strain and condition to compare the effect of salt and pH on the swimming speeds of *V. cholerae*  $\Delta pomAB$  cells expressing wild type PomB-Strep, or its S26T or S26A variants. With cells expressing wild type stator complexes, the highest velocities (top speed as well as average and median speed of the fast swimmer classes), and the second largest number of fast swimmers, were observed at pH 8.0 in the presence of 11 mM Na<sup>+</sup> and 183 mM K<sup>+</sup> (Fig 6, and S2–S4 Tables). High Na<sup>+</sup> (182 mM, with 12 mM K<sup>+</sup>) was inhibitory, since the lowest numbers (29 at pH 8.0, 18 at pH 9.0) of fast swimmers were observed under this condition of salt. Without any added salt, the numbers of fast swimmers at pH 8.0 or 9.0 lay between the numbers observed with LB-Na<sup>+</sup> and LB-K<sup>+</sup> (Fig 6, and S2–S4 Tables). This is in accord with our previous findings that the increase in osmolality (due to added chloride salts) rather than the increase in Na<sup>+</sup> concentration promoted motility of *V. cholerae* cells overexpressing wild type stator complexes [52]. Chloride, a chaotropic anion, might distort the local water structure within the Na<sup>+</sup> access channel of the PomA<sub>4</sub>PomB<sub>2</sub> stator, partially disrupting the hydration shell of Na<sup>+</sup>, and facilitating its passage through the channel. We next focused on the results obtained with *V. cholerae* cells at pH 7.0 since this was the pH chosen for the *V. alginolyticus* study addressing the effect of the PomB-S27T mutation [53]. Fast swimmers were detected among the *V. cholerae*  $\Delta pomAB$  cells expressing wild type PomB-Strep under all salt conditions tested (182 mM Na<sup>+</sup>/12 mM K<sup>+</sup>, 11 mM Na<sup>+</sup>/12 mM K<sup>+</sup>, or 11 mM Na<sup>+</sup>/183 mM K<sup>+</sup>). With cells expressing the PomB-S26T-Strep variant, the ability for fast swimming (41  $\mu\text{m s}^{-1}$  or faster) was lost under all salt conditions at pH 7.0. Raising the pH to 9.0 rescued cells producing PomB-S26T-Strep, enabling them for fast swimming under all salt concentrations studied (Fig 6), with distributions of velocities similar to wild type cells. However, at pH 8.0, the presence of salt became critical for the stator containing the PomB-S26T-Strep variant. Fast swimming of cells required the presence of either 182 mM Na<sup>+</sup>/12 mM K<sup>+</sup> or 11 mM Na<sup>+</sup>/183 mM K<sup>+</sup>. At 11 mM Na<sup>+</sup>/12 mM K<sup>+</sup> (LB without added salt), no fast swimmers were observed at all (Fig 6, and S2–S4 Tables). When S26 was replaced by alanine, fast swimming cells (comparable to the wild type) were observed at pH 7.0, 8.0 and 9.0 at low salt (11 mM Na<sup>+</sup>/12 mM K<sup>+</sup>) or high Na<sup>+</sup> (182 mM Na<sup>+</sup>/12 mM K<sup>+</sup>), but not at high K<sup>+</sup> (11 mM Na<sup>+</sup>/183 mM K<sup>+</sup>) with pH 7.0 or 8.0. Only at pH 9.0, cells possessing the PomB-S26A-Strep variant exhibited fast swimming despite the presence of 183 mM K<sup>+</sup> (Fig 6).

### Formation of transmembrane voltage in *V. cholerae* $\Delta pomAB$ expressing PomB and its S26A or S26T variants

Overexpression resulted in the accumulation of pre-assembled stators in the inner membrane of *V. cholerae* [52]. Unspecific ion flux – especially when introducing mutations within the channel region of the stators – should be considered as this might dissipate the sodium-motive force across the inner membrane. This in turn could affect flagellar rotation. The MotA<sub>4</sub>-MotB<sub>2</sub> stators of the proton-dependent flagella of *E. coli* and *Salmonella*, as well as the PomA<sub>4</sub>PomB<sub>2</sub> stators of the sodium-dependent flagella of *V. alginolyticus*, assume a

“plugged” confirmation in their pre-assembled state and therefore do not promote ion flux prior to insertion into the flagellar motor [60–65]. To exclude that the overexpressed stators containing PomB variants led to a decrease in the sodium-motive force, the transmembrane voltage established by the different *V. cholerae* strains was determined. As a control, *V. cholerae*  $\Delta nqr$  lacking the  $\text{Na}^+$ -translocating NADH:quinone oxidoreductase ( $\text{Na}^+$ -NQR) was included in the analysis. The  $\text{Na}^+$ -NQR is an electrogenic NADH dehydrogenase in the respiratory chain of *V. cholerae* and represents the main generator of the sodium-motive force [66]. Cells were grown in LB medium at the indicated conditions, and expression of wild type PomB-Strep, PomB-S26A-Strep or PomB-S26T-Strep in the *V. cholerae*  $\Delta pomAB$  host was induced by adding 10 mM L-arabinose. The *V. cholerae*  $\Delta nqr$  strain devoid of the  $\text{Na}^+$ -NQR was included to demonstrate that a decrease in membrane potential was readily detected with the BacLight assay. This deletion strain lacks its respiratory  $\text{Na}^+$  pump which contributes to the formation of a transmembrane voltage and a chemical  $\text{Na}^+$  gradient in *V. cholerae*. Yet, *V. cholerae*  $\Delta nqr$  is viable and motile, and contains all flagellar genes [67]. With all PomB variants studied, and under all conditions of salt and pH investigated, the transmembrane voltage established by *V. cholerae* strains overproducing  $\text{PomA}_4\text{B}_2$  stator complexes was always higher than the transmembrane voltage established by the *nqr* deletion strain (Fig 7). We conclude that the presence of pre-assembled stator complexes in the inner membrane [52] did not diminish the sodium-motive force by passive influx of  $\text{Na}^+$  into the cell. The transmembrane voltage established by *V. cholerae*  $\Delta pomAB$  expressing the

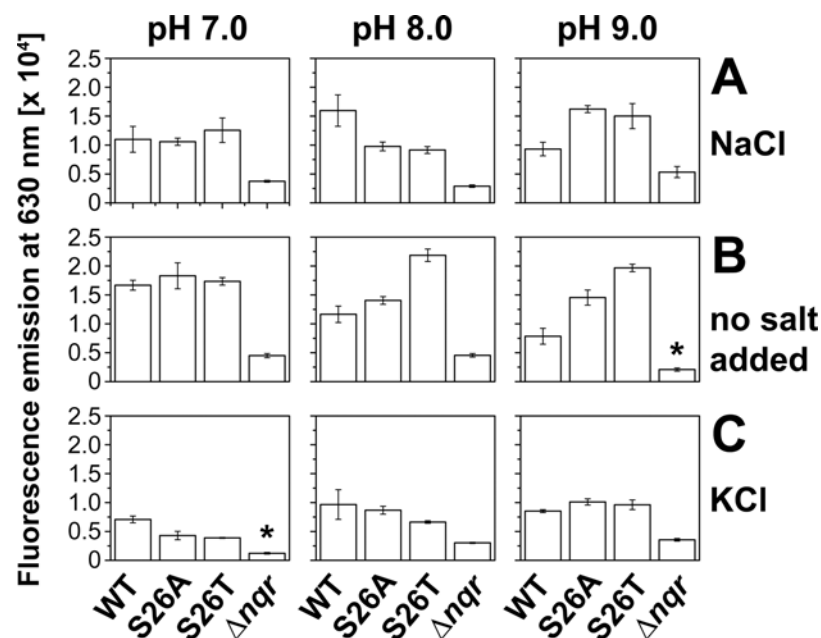


**Fig 7. Influence of pH and salt condition on the membrane potential generated by *V. cholerae*  $\Delta pomAB$  cells overproducing His<sub>6</sub>-PomA together with PomB-S26T-Strep.** The fluorescence emission of the fluorophore DiOC<sub>2</sub> at 630 nm was determined to estimate the formation of membrane potential,  $\Delta\Psi$  (inside negative). Average values and standard deviations of three biological replicates, each from a different culture, are presented. *V. cholerae*  $\Delta nqr$  lacks the  $\text{Na}^+$ -translocating NADH:quinone oxidoreductase and is impaired in the formation of  $\Delta\Psi$ . The asterisks indicate conditions which allow only poor growth of *V. cholerae*  $\Delta nqr$ , impairing determination of  $\Delta\Psi$ . A: LB- $\text{Na}^+$ ; B: no salt added, with residual concentrations of 11 mM  $\text{Na}^+$  and 12 mM  $\text{K}^+$ ; C: LB- $\text{K}^+$ .

doi:10.1371/journal.pone.0123518.g007



PomB-S26A-Strep or PomB-S26T-Strep did not significantly differ from  $\Delta\Psi$  established by cells expressing wild type PomB-Strep. It is noteworthy that at pH 7.0, the S26T variant did not confer any drastic change in  $\Delta\Psi$  under every salt condition tested when compared to wild type PomB-Strep, but was clearly impaired in motility (Fig 6). High  $K^+$  at pH 7.0 or 8.0 was inhibitory for fast swimming in the PomB-S26A-Strep variant (Fig 6), but cells expressing PomB-S26A-Strep were not compromised in  $\Delta\Psi$  formation under these conditions. In summary, we demonstrated that introducing mutations did not affect the expression level of PomB-Strep, and did not diminish the transmembrane voltage required to drive flagellar rotation. The effects of mutations in PomB on motility described here therefore resulted from altered cation transport properties of the PomA<sub>4</sub>B<sub>2</sub> complex as part of the flagellar motor.

## Discussion

The PomA<sub>4</sub>PomB<sub>2</sub> complex of the polar flagellum of *V. cholerae* provides at least one pathway for the transport of  $Na^+$  from the periplasm to the cytoplasm along the electrochemical  $Na^+$  gradient. This so-called stator complex is an essential part of the motor, since the flux of  $Na^+$  through PomA<sub>4</sub>PomB<sub>2</sub> is a prerequisite for rotation of flagellum [6,52,59,68] (Fig 1). The terms “ $Na^+$  transport” or “ $Na^+$  flux” suggest different mechanisms of stator function. Does PomA<sub>4</sub>PomB<sub>2</sub> represent a  $Na^+$  transporter (or pump) with a distinct binding site for  $Na^+$ , exemplified by the  $F_o$  part of the  $Na^+$ -translocating  $F_1F_o$  ATP synthase [69]? Or does it bear similarity to a channel designed for the fast flux of cations, an example being the  $K^+$  channel [70]? Assuming that the stator complex possesses a critical carboxylate required as a ligand for  $Na^+$  in a binding site, as found in the  $F_o$  part of the ATP synthase, one would expect a competition between  $Na^+$  and  $H^+$  for binding to this carboxylate. Increasing the pH would promote flagellar rotation at a fixed  $Na^+$  concentration. On the other hand, increasing the  $Na^+$  concentration at a given pH should prevent protonation of the critical carboxylate. However, with the  $Na^+$ -dependent flagellum from *V. cholerae*, rotation was enhanced by a raise in external proton concentration, and  $Na^+$  did not prevent the protonation of membrane-embedded carboxylates, indicated by the covalent modification of the carboxylic groups with carbodiimide [52]. These and other findings pointed against a direct binding of  $Na^+$  to the critical, membrane-embedded D23 in PomB. A direct binding of  $Na^+$  was previously proposed for the corresponding D24 in the related PomB from *V. alginolyticus* [71]. Yet doubtlessly, this strictly conserved aspartate in PomB plays an important role during  $Na^+$  transport. Replacing D23 in *V. cholerae* PomB with asparagine, or the corresponding D24 in *V. alginolyticus* PomB with asparagine or cysteine, completely blocks flagellar rotation [29,30,40,52]. In the PomA wild type background, the presence of a carboxyl group (provided by Asp or Glu) at this position in PomB is essential for motor function [29,52,72]. By studying the motility behavior of *V. cholerae* expressing different variants of PomB under different conditions of salt and pH in softagar plates, we proposed that D23 and S26 in the membrane-embedded stretch of PomB contribute to the formation of a hydrogen bond network which is essential for passage of  $Na^+$  through the stator [52]. Our results suggested that the protonation of D23, or its interaction with water or hydronium ions, is still possible despite the presence of  $Na^+$  [52]. The specificity of the PomA<sub>4</sub>PomB<sub>2</sub> stator for  $Na^+$  implies that at a certain step in the transport process, the cation must become at least partially dehydrated [70]. Otherwise, the stator complex could not discriminate  $Na^+$  from other cations, like  $K^+$ . Once the water molecules are (partially) removed, the PomA<sub>4</sub>PomB<sub>2</sub> stator may offer distinct binding site(s) which satisfy the need of the sodium ion with respect to its coordination geometry (if operating as a pump). Alternatively, the stator may provide a selectivity filter, which only allows passage of the (at least partially dehydrated) sodium ion (if operating as a

channel) [70,73]. Berry and coworkers [58] studied the performance of flagellum rotation in *E. coli* using a chimeric stator providing specificity towards  $\text{Na}^+$  (and not  $\text{H}^+$ ) as coupling ion for the flagellar motor. *E. coli* cells were fixed to a glass surface, and motor rotation was observed via back-focal-plane interferometry of beads attached to a single, truncated flagellar filament. Using a low-expression vector for stator production, authors of that study observed distributions of rotational speeds which were presented in histograms. It was assumed that the distinct rotational frequencies resulted from different numbers of stator complexes integrated in the flagellar motor of the particular cell studied, and the slowest major peak in each histogram was assigned to the rotational frequency of a flagellar motor equipped with one, single stator unit [58]. In our investigations, we chose a high-expression system for the  $\text{Na}^+$ -dependent stator from *V. cholerae* studied in complex with its endogenous flagellar motor in *V. cholerae*, focusing on the fast swimmers which operate flagella with maximum occupancy of stator complexes. These fast swimmers were only observed with overproduced stator complexes, and enabled us to study the influence of pH and salt composition of the medium on the performance of stators containing wild type PomB (fused to a Strep tag), or variants carrying mutations in PomB-Strep. S26 within the single transmembrane helix of PomB was critical for fast rotation of the flagellum under a broad range of physiological  $\text{H}^+$  and salt concentrations. Removal of the hydroxyl group at this position (S26A), or even maintaining the OH-group, but at a slightly different position (S26T), strongly impaired fast swimming of *V. cholerae* cells, but in a pH- and salt-dependent manner. Homma and coworkers (2011) studied the effect of the corresponding S27T mutation in PomB of *V. alginolyticus* and observed some contribution of S27T to rotor function in the presence of 200 mM  $\text{Na}^+$  [53]. With *V. cholerae*, cells expressing the PomB-S26T-Strep variant were clearly slowed down compared to cells with wild type PomB-Strep at pH 7.0, but regained the ability for fast swimming at pH 9.0. This strong effect is difficult to reconcile with different protonation states of the OH-groups in serine or threonine residues at a given pH in the range from 7.0 to 9.0, since the  $\text{pK}_a$  of the hydroxyl group in both amino acids is too high (>13) to expect deprotonated states. Instead, the observed effects of salt and  $\text{H}^+$  concentrations on stator function could be due to a rearrangement of water molecules or hydrogen bonds within the water-filled access channel of the stator complex (Fig 8). A helical wheel prediction of PomB suggests that S26 resides on the same side as the critical D23 and faces the inside of a transmembrane channel built by PomA<sub>4</sub>PomB<sub>2</sub> [32,52]. D23 is positioned below S26 when viewed from the periplasmic side of the inner membrane (Fig 8). It is proposed that S26, together with D23, is important for fast transport through the stator channel by perturbing the hydration shell of  $\text{Na}^+$ , preparing it for passage through a selectivity filter located below D23. This constriction in the passageway for the  $\text{Na}^+$  will not depend on the presence of charged amino acid side chains as long as the critical diameter is maintained which is selective for dehydrated  $\text{Na}^+$  (Fig 8). This model would be consistent with the finding that studies with chimeric stators made up of domains from subunits derived from  $\text{H}^+$ - or  $\text{Na}^+$ -dependent stators so far failed to identify critical amino acids conferring cation selectivity [24]. It should be noted that D23 could also be part of the selectivity filter which might accommodate a partially hydrated  $\text{Na}^+$ , as proposed for the bacterial  $\text{Na}^+$  channel [73]. This scenario cannot unequivocally be excluded by our findings. In summary, we demonstrated that S26 is crucial to promote fast rotation of the flagellum by facilitating sodium ion transport across the cell membrane. Our results indicate that S26 does not directly interact with  $\text{Na}^+$  but rather affects its hydration shell. S26 of PomB is important for  $\text{Na}^+$  flux through PomA<sub>4</sub>B<sub>2</sub> under very different conditions of salinity and pH, and guarantees motility of *V. cholerae* in low- and high-salinity environments [74] inhabited by this versatile pathogen.

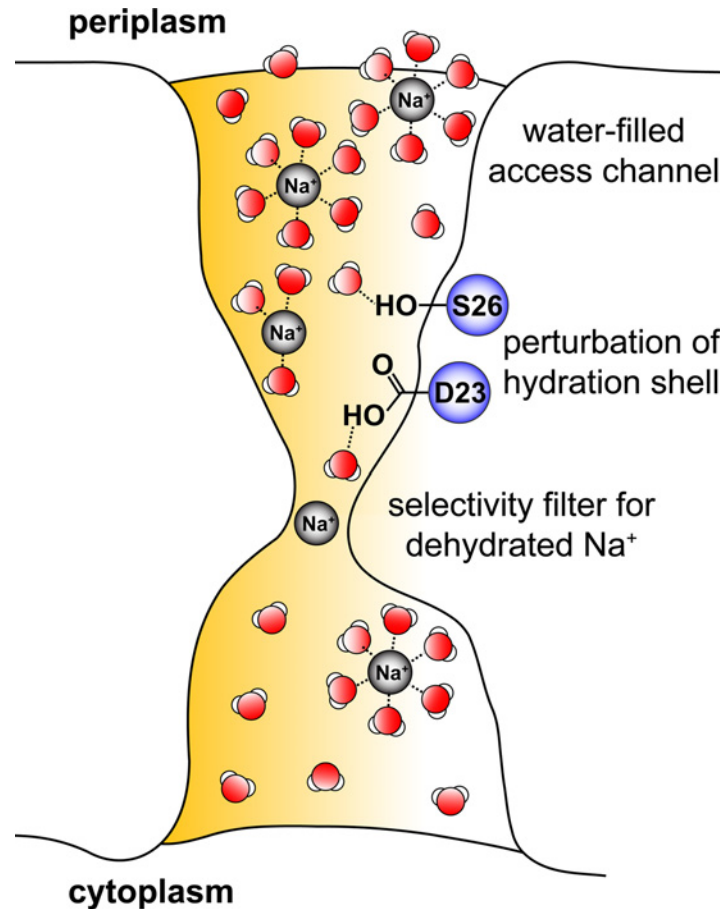


**Fig 8. Na<sup>+</sup> flux through the flagellar PomA<sub>4</sub>PomB<sub>2</sub> complex by a channel-like mechanism.** Na<sup>+</sup> enters the PomA<sub>4</sub>PomB<sub>2</sub> stator complex in its hydrated state from the periplasm via a water-filled access channel. The conserved amino acid residues S26 and D23 within the membrane-bound region of PomB interact with water molecules surrounding the central Na<sup>+</sup>, hereby perturbing its hydration shell. The sodium ion passes the narrow constriction site, or selectivity filter, in its dehydrated state. After passage through the filter, Na<sup>+</sup> is hydrated and released towards the cytoplasmic side of the stator. The downhill flux of Na<sup>+</sup> from the periplasm to the cytoplasm is driven by the electrochemical Na<sup>+</sup> gradient across the inner membrane.

doi:10.1371/journal.pone.0123518.g008

## Supporting Information

**S1 Table. Statistical analyses of tracks from *V. cholerae* reference strain and *V. cholerae*  $\Delta pomAB$  transformed with pAB coding for His<sub>6</sub>-pomA and pomB-Strep.** Velocities were determined in LB medium with 171 mM Na<sup>+</sup> added. At pH 7.0, 8.0 and 9.0, the total numbers of tracks recorded with the *V. cholerae* reference strain were 305, 326 and 320, and with *V. cholerae*  $\Delta pomAB$  expressing His<sub>6</sub>-PomA and wild type PomB-Strep 323, 316 and 322, respectively. SD: Standard deviation.  
(PDF)

**S2 Table. Statistical analyses of tracks from *V. cholerae*  $\Delta pomAB$  cells overproducing His<sub>6</sub>-PomA together with PomB-Strep, PomB-S26A-Strep or PomB-S26T-Strep in LB medium with 171 mM Na<sup>+</sup> added.** At pH 7.0, 8.0 and 9.0, the total numbers of tracks recorded with *V. cholerae*  $\Delta pomAB$  expressing His<sub>6</sub>-PomA and wild type PomB-Strep were 629, 641 and 650, respectively. For His<sub>6</sub>-PomA together with PomB-S26A-Strep, the numbers of tracks were 650,

647 and 650, respectively, and 650, 650 and 650 for His<sub>6</sub>-PomA together with PomB-S26T-Strep. SD: Standard deviation.

(PDF)

**S3 Table. Statistical analyses of tracks from *V. cholerae*  $\Delta pomAB$  cells overproducing His<sub>6</sub>-PomA together with PomB-Strep, PomB-S26A-Strep or PomB-S26T-Strep in LB medium without added salt.** At pH 7.0, 8.0 and 9.0, the total numbers of tracks recorded with *V. cholerae*  $\Delta pomAB$  expressing His<sub>6</sub>-PomA and wild type PomB-Strep were 650, 650 and 649, respectively. For His<sub>6</sub>-PomA together with PomB-S26A-Strep, the numbers of tracks were 650, 650 and 649, respectively, and 650, 677 and 650 for His<sub>6</sub>-PomA together with PomB-S26T-Strep. SD: Standard deviation.

(PDF)

**S4 Table. Statistical analyses of tracks from *V. cholerae*  $\Delta pomAB$  cells overproducing His<sub>6</sub>-PomA together with PomB-Strep, PomB-S26A-Strep or PomB-S26T-Strep in LB medium with 171 mM K<sup>+</sup> added.** At pH 7.0, 8.0 and 9.0, the total numbers of tracks recorded with *V. cholerae*  $\Delta pomAB$  expressing His<sub>6</sub>-PomA and wild type PomB-Strep were 649, 631 and 650, respectively. For His<sub>6</sub>-PomA together with PomB-S26A-Strep, the numbers of tracks were 640, 659 and 650, respectively, and 650, 650 and 650 for His<sub>6</sub>-PomA together with PomB-S26T-Strep. SD: Standard deviation.

(PDF)

## Acknowledgments

We thank Claudia Häse (Oregon State University) for providing the *V. cholerae*  $\Delta pomAB$  and *V. cholerae*  $\Delta nqr$  strains.

## Author Contributions

Conceived and designed the experiments: PH TV JS. Performed the experiments: PH TV. Analyzed the data: PH TV JS. Contributed reagents/materials/analysis tools: JS. Wrote the paper: PH TV JS.

## References

1. Armitage JP. Bacterial tactic responses. *Adv Microb Physiol.* 1999; 41: 229–289. PMID: [10500847](#)
2. Fenchel T. Microbial behavior in a heterogeneous world. *Science* 2002; 296: 1068–1071. PMID: [12004118](#)
3. Berg HC. The rotary motor of bacterial flagella. *Annu Rev Biochem.* 2003; 72: 19–54. PMID: [12500982](#)
4. Li N, Kojima S, Homma M. Sodium-driven motor of the polar flagellum in marine bacteria *Vibrio*. *Genes Cells* 2011; 16: 985–999. doi: [10.1111/j.1365-2443.2011.01545.x](#) PMID: [21895888](#)
5. Morimoto YV, Minamino T. Structure and function of the bi-directional bacterial flagellar motor. *Biomolecules* 2014; 4: 217–234. doi: [10.3390/biom4010217](#) PMID: [24970213](#)
6. Imae Y, Atsumi T. Na<sup>+</sup>-driven bacterial flagellar motors. *J Bioenerg Biomembr.* 1989; 21: 705–716. PMID: [2687262](#)
7. Manson MD, Tedesco P, Berg HC, Harold FM, Van der Drift C. A protonmotive force drives bacterial flagella. *Proc Natl Acad Sci U S A.* 1977; 74: 3060–3064. PMID: [19741](#)
8. Larsen SH, Adler J, Gargus JJ, Hogg RW. Chemomechanical coupling without ATP: the source of energy for motility and chemotaxis in bacteria. *Proc Natl Acad Sci U S A.* 1974; 71: 1239–1243. PMID: [4598295](#)
9. Glagolev AN, Skulachev VP. The proton pump is a molecular engine of motile bacteria. *Nature* 1978; 272: 280–282. PMID: [24186](#)
10. Blair DF, Berg HC. The MotA protein of *E. coli* is a proton-conducting component of the flagellar motor. *Cell* 1990; 60: 439–449. PMID: [2154333](#)

11. Sharp LL, Zhou J, Blair DF. Features of MotA proton channel structure revealed by tryptophan-scanning mutagenesis. *Proc Natl Acad Sci U S A*. 1995; 92: 7946–7950. PMID: [7644518](#)
12. Stolz B, Berg HC. Evidence for interactions between MotA and MotB, torque-generating elements of the flagellar motor of *Escherichia coli*. *J Bacteriol*. 1991; 173: 7033–7037. PMID: [1938906](#)
13. Tang H, Braun TF, Blair DF. Motility protein complexes in the bacterial flagellar motor. *J Mol Biol*. 1996; 261: 209–221. PMID: [8757288](#)
14. Kojima S, Blair DF. Solubilization and purification of the MotA/MotB complex of *Escherichia coli*. *Biochemistry* 2004; 43: 26–34. PMID: [14705928](#)
15. McCarter LL. Polar flagellar motility of the *Vibrionaceae*. *Microbiol Mol Biol Rev*. 2001; 65: 445–462. PMID: [11528005](#)
16. Yorimitsu T, Sato K, Asai Y, Kawagishi I, Homma M. Functional interaction between PomA and PomB, the Na<sup>+</sup>-driven flagellar motor components of *Vibrio alginolyticus*. *J Bacteriol*. 1999; 181: 5103–5106. PMID: [10438787](#)
17. Sato K, Homma M. Functional reconstitution of the Na<sup>+</sup>-driven polar flagellar motor component of *Vibrio alginolyticus*. *J Biol Chem*. 2000; 275: 5718–5722. PMID: [10681557](#)
18. Asai Y, Kojima S, Kato H, Nishioka N, Kawagishi I, Homma M. Putative channel components for the fast-rotating sodium-driven flagellar motor of a marine bacterium. *J Bacteriol*. 1997; 179: 5104–5110. PMID: [9260952](#)
19. Sato K, Homma M. Multimeric structure of PomA, a component of the Na<sup>+</sup>-driven polar flagellar motor of *Vibrio alginolyticus*. *J Biol Chem*. 2000; 275: 20223–20228. PMID: [10783392](#)
20. Asai Y, Kawagishi I, Sockett RE, Homma M. Hybrid motor with H<sup>+</sup>- and Na<sup>+</sup>-driven components can rotate *Vibrio* polar flagella by using sodium ions. *J Bacteriol*. 1999; 181: 6332–6338. PMID: [10515922](#)
21. Asai Y, Yakushi T, Kawagishi I, Homma M. Ion-coupling determinants of Na<sup>+</sup>-driven and H<sup>+</sup>-driven flagellar motors. *J Mol Biol*. 2003; 327: 453–463. PMID: [12628250](#)
22. Gosink KK, Håse CC. Requirements for conversion of the Na<sup>+</sup>-driven flagellar motor of *Vibrio cholerae* to the H<sup>+</sup>-driven motor of *Escherichia coli*. *J Bacteriol*. 2000; 182: 4234–4240. PMID: [10894732](#)
23. Sowa Y, Rowe AD, Leake MC, Yakushi T, Homma M, Ishijima A, et al. Direct observation of steps in rotation of the bacterial flagellar motor. *Nature* 2005; 437: 916–919. PMID: [16208378](#)
24. Sowa Y, Berry RM. Bacterial flagellar motor. *Q Rev Biophys*. 2008; 41: 103–132. doi: [10.1017/S0033583508004691](#) PMID: [18812014](#)
25. Paulick A, Koerdt A, Lassak J, Huntley S, Wilms I, Narberhaus F, et al. Two different stator systems drive a single polar flagellum in *Shewanella oneidensis* MR-1. *Mol Microbiol*. 2009; 71: 836–850. doi: [10.1111/j.1365-2958.2008.06570.x](#) PMID: [19170881](#)
26. Terahara N, Krulwich TA, Ito M. Mutations alter the sodium versus proton use of a *Bacillus clausii* flagellar motor and confer dual ion use on *Bacillus subtilis* motors. *Proc Natl Acad Sci U S A*. 2008; 105: 14359–14364. doi: [10.1073/pnas.0802106105](#) PMID: [18796609](#)
27. Terahara N, Sano M, Ito M. A *Bacillus* flagellar motor that can use both Na<sup>+</sup> and K<sup>+</sup> as a coupling ion is converted by a single mutation to use only Na<sup>+</sup>. *PLoS One* 2012; 7: e46248. doi: [10.1371/journal.pone.0046248](#) PMID: [23049994](#)
28. Kojima S, Yamamoto K, Kawagishi I, Homma M. The polar flagellar motor of *Vibrio cholerae* is driven by an Na<sup>+</sup> motive force. *J Bacteriol*. 1999; 181: 1927–1930. PMID: [10074090](#)
29. Vorburger T, Stein A, Ziegler U, Kaim G, Steuber J. Functional role of a conserved aspartic acid residue in the motor of the Na<sup>+</sup>-driven flagellum from *Vibrio cholerae*. *Biochim Biophys Acta* 2009; 1787: 1198–1204. doi: [10.1016/j.bbabi.2009.05.015](#) PMID: [19501041](#)
30. Yakushi T, Maki S, Homma M. Interaction of PomB with the third transmembrane segment of PomA in the Na<sup>+</sup>-driven polar flagellum of *Vibrio alginolyticus*. *J Bacteriol*. 2004; 186: 5281–5291. PMID: [15292129](#)
31. Braun TF, Al-Mawsawi LQ, Kojima S, Blair DF. Arrangement of core membrane segments in the MotA/MotB proton-channel complex of *Escherichia coli*. *Biochemistry* 2004; 43: 35–45. PMID: [14705929](#)
32. Kim EA, Price-Carter M, Carlquist WC, Blair DF. Membrane segment organization in the stator complex of the flagellar motor: implications for proton flow and proton-induced conformational change. *Biochemistry* 2008; 47: 11332–11339. doi: [10.1021/bi801347a](#) PMID: [18834143](#)
33. Braun TF, Blair DF. Targeted disulfide cross-linking of the MotB protein of *Escherichia coli*: evidence for two H<sup>+</sup> channels in the stator complex. *Biochemistry* 2001; 40: 13051–13059. PMID: [11669643](#)
34. Che YS, Nakamura S, Kojima S, Kami-ike N, Namba K, Minamino T. Suppressor analysis of the MotB (D33E) mutation to probe bacterial flagellar motor dynamics coupled with proton translocation. *J Bacteriol*. 2008; 190: 6660–6667. doi: [10.1128/JB.00503-08](#) PMID: [18723617](#)
35. Berg HC. Dynamic properties of bacterial flagellar motors. *Nature* 1974; 249: 77–79. PMID: [4598032](#)



36. Zhu S, Takao M, Li N, Sakuma M, Nishino Y, Homma M, et al. Conformational change in the periplasmic region of the flagellar stator coupled with the assembly around the rotor. *Proc Natl Acad Sci U S A*. 2014; 111: 13523–13528. doi: [10.1073/pnas.1324201111](https://doi.org/10.1073/pnas.1324201111) PMID: [25197056](https://pubmed.ncbi.nlm.nih.gov/25197056/)
37. Leake MC, Chandler JH, Wadhams GH, Bai F, Berry RM, Armitage JP. Stoichiometry and turnover in single, functioning membrane protein complexes. *Nature* 2006; 443: 355–358. PMID: [16971952](https://pubmed.ncbi.nlm.nih.gov/16971952/)
38. Reid SW, Leake MC, Chandler JH, Lo CJ, Armitage JP, Berry RM. The maximum number of torque-generating units in the flagellar motor of *Escherichia coli* is at least 11. *Proc Natl Acad Sci U S A*. 2006; 103: 8066–8071. PMID: [16698936](https://pubmed.ncbi.nlm.nih.gov/16698936/)
39. Magariyama Y, Sugiyama S, Muramoto K, Maekawa Y, Kawagishi I, Imae Y, et al. Very fast flagellar rotation. *Nature* 1994; 371: 752. PMID: [7935835](https://pubmed.ncbi.nlm.nih.gov/7935835/)
40. Fukuoka H, Wada T, Kojima S, Ishijima A, Homma M. Sodium-dependent dynamic assembly of membrane complexes in sodium-driven flagellar motors. *Mol Microbiol*. 2009; 71: 825–835. doi: [10.1111/j.1365-2958.2008.06569.x](https://doi.org/10.1111/j.1365-2958.2008.06569.x) PMID: [19183284](https://pubmed.ncbi.nlm.nih.gov/19183284/)
41. Van Way SM, Hosking ER, Braun TF, Manson MD. Mot protein assembly into the bacterial flagellum: a model based on mutational analysis of the *motB* gene. *J Mol Biol*. 2000; 297: 7–24. PMID: [10704303](https://pubmed.ncbi.nlm.nih.gov/10704303/)
42. Kojima S, Blair DF. Conformational change in the stator of the bacterial flagellar motor. *Biochemistry* 2001; 40: 13041–13050. PMID: [11669642](https://pubmed.ncbi.nlm.nih.gov/11669642/)
43. Lloyd SA, Whitby FG, Blair DF, Hill CP. Structure of the C-terminal domain of FliG, a component of the rotor in the bacterial flagellar motor. *Nature* 1999; 400: 472–475. PMID: [10440379](https://pubmed.ncbi.nlm.nih.gov/10440379/)
44. Yorimitsu T, Mimaki A, Yakushi T, Homma M. The conserved charged residues of the C-terminal region of FliG, a rotor component of the Na<sup>+</sup>-driven flagellar motor. *J Mol Biol*. 2003; 334: 567–583. PMID: [14623195](https://pubmed.ncbi.nlm.nih.gov/14623195/)
45. Zhou J, Blair DF. Residues of the cytoplasmic domain of MotA essential for torque generation in the bacterial flagellar motor. *J Mol Biol*. 1997; 273: 428–439. PMID: [9344750](https://pubmed.ncbi.nlm.nih.gov/9344750/)
46. Zhou J, Lloyd SA, Blair DF. Electrostatic interactions between rotor and stator in the bacterial flagellar motor. *Proc Natl Acad Sci U S A*. 1998; 95: 6436–6441. PMID: [9600984](https://pubmed.ncbi.nlm.nih.gov/9600984/)
47. Lloyd SA, Blair DF. Charged residues of the rotor protein FliG essential for torque generation in the flagellar motor of *Escherichia coli*. *J Mol Biol*. 1997; 266: 733–744. PMID: [9102466](https://pubmed.ncbi.nlm.nih.gov/9102466/)
48. Yorimitsu T, Sowa Y, Ishijima A, Yakushi T, Homma M. The systematic substitutions around the conserved charged residues of the cytoplasmic loop of Na<sup>+</sup>-driven flagellar motor component PomA. *J Mol Biol*. 2002; 320: 403–413. PMID: [12079395](https://pubmed.ncbi.nlm.nih.gov/12079395/)
49. Morimoto YV, Nakamura S, Kami-ike N, Namba K, Minamino T. Charged residues in the cytoplasmic loop of MotA are required for stator assembly into the bacterial flagellar motor. *Mol Microbiol*. 2010; 78: 1117–1129. doi: [10.1111/j.1365-2958.2010.07391.x](https://doi.org/10.1111/j.1365-2958.2010.07391.x) PMID: [21091499](https://pubmed.ncbi.nlm.nih.gov/21091499/)
50. Morimoto YV, Nakamura S, Hiraoka KD, Namba K, Minamino T. Distinct roles of highly conserved charged residues at the MotA-FliG interface in bacterial flagellar motor rotation. *J Bacteriol*. 2013; 195: 474–481. doi: [10.1128/JB.01971-12](https://doi.org/10.1128/JB.01971-12) PMID: [23161029](https://pubmed.ncbi.nlm.nih.gov/23161029/)
51. Takekawa N, Kojima S, Homma M. Contribution of many charged residues at the stator-rotor interface of the Na<sup>+</sup>-driven flagellar motor to torque generation in *Vibrio alginolyticus*. *J Bacteriol*. 2014; 196: 1377–1385. doi: [10.1128/JB.01392-13](https://doi.org/10.1128/JB.01392-13) PMID: [24464458](https://pubmed.ncbi.nlm.nih.gov/24464458/)
52. Halang P, Leptihn S, Meier T, Vorburger T, Steuber J. The function of the Na<sup>+</sup>-driven flagellum of *Vibrio cholerae* is determined by osmolality and pH. *J Bacteriol*. 2013; 195: 4888–4899. doi: [10.1128/JB.00353-13](https://doi.org/10.1128/JB.00353-13) PMID: [23974033](https://pubmed.ncbi.nlm.nih.gov/23974033/)
53. Terauchi T, Terashima H, Kojima S, Homma M. A conserved residue, PomB-F22, in the transmembrane segment of the flagellar stator complex, has a critical role in conducting ions and generating torque. *Microbiology* 2011; 157: 2422–2432. doi: [10.1099/mic.0.048488-0](https://doi.org/10.1099/mic.0.048488-0) PMID: [21636648](https://pubmed.ncbi.nlm.nih.gov/21636648/)
54. Mekalanos JJ, Swartz DJ, Pearson GD, Harford N, Groyne F, de Wilde M. Cholera toxin genes: nucleotide sequence, deletion analysis and vaccine development. *Nature* 1983; 306: 551–557. PMID: [6646234](https://pubmed.ncbi.nlm.nih.gov/6646234/)
55. Barquera B, Hellwig P, Zhou W, Morgan JE, Hase CC, Gosink KK, et al. Purification and characterization of the recombinant Na<sup>+</sup>-translocating NADH:quinone oxidoreductase from *Vibrio cholerae*. *Biochemistry* 2002; 41: 3781–3789. PMID: [11888296](https://pubmed.ncbi.nlm.nih.gov/11888296/)
56. Underwood SA, Buszko ML, Shanmugam KT, Ingram LO. Lack of protective osmolytes limits final cell density and volumetric productivity of ethanologenic *Escherichia coli* KO11 during xylose fermentation. *Appl Environ Microbiol*. 2004; 70: 2734–2740. PMID: [15128526](https://pubmed.ncbi.nlm.nih.gov/15128526/)
57. Neidhardt FC, Ingraham JL, Curtiss III R, Lin ECC, Brooks Low K, Magasanik B, et al. *Escherichia coli* and *Salmonella typhimurium*: cellular and molecular biology. Washington, D.C.: American Society for Microbiology; 1996.

58. Lo CJ, Sowa Y, Pilizota T, Berry RM. Mechanism and kinetics of a sodium-driven bacterial flagellar motor. *Proc Natl Acad Sci U S A*. 2013; 110: E2544–2551. doi: [10.1073/pnas.1301664110](https://doi.org/10.1073/pnas.1301664110) PMID: [23788659](https://pubmed.ncbi.nlm.nih.gov/23788659/)
59. Thormann KM, Paulick A. Tuning the flagellar motor. *Microbiology* 2010; 156: 1275–1283. doi: [10.1099/mic.0.029595-0](https://doi.org/10.1099/mic.0.029595-0) PMID: [20203052](https://pubmed.ncbi.nlm.nih.gov/20203052/)
60. Wilson ML, Macnab RM. Co-overproduction and localization of the *Escherichia coli* motility proteins *motA* and *motB*. *J Bacteriol*. 1990; 172: 3932–3939. PMID: [2193926](https://pubmed.ncbi.nlm.nih.gov/2193926/)
61. Hosking ER, Vogt C, Bakker EP, Manson MD. The *Escherichia coli* MotAB proton channel unplugged. *J Mol Biol*. 2006; 364: 921–937. PMID: [17052729](https://pubmed.ncbi.nlm.nih.gov/17052729/)
62. Kojima S, Imada K, Sakuma M, Sudo Y, Kojima C, Minamino T, et al. Stator assembly and activation mechanism of the flagellar motor by the periplasmic region of MotB. *Mol Microbiol*. 2009; 73: 710–718. doi: [10.1111/j.1365-2958.2009.06802.x](https://doi.org/10.1111/j.1365-2958.2009.06802.x) PMID: [19627504](https://pubmed.ncbi.nlm.nih.gov/19627504/)
63. Li N, Kojima S, Homma M. Characterization of the periplasmic region of PomB, a Na<sup>+</sup>-driven flagellar stator protein in *Vibrio alginolyticus*. *J Bacteriol*. 2011; 193: 3773–3784. doi: [10.1128/JB.00113-11](https://doi.org/10.1128/JB.00113-11) PMID: [21602350](https://pubmed.ncbi.nlm.nih.gov/21602350/)
64. Takekawa N, Terauchi T, Morimoto YV, Minamino T, Lo CJ, Kojima S, et al. Na<sup>+</sup> conductivity of the Na<sup>+</sup>-driven flagellar motor complex composed of unplugged wild-type or mutant PomB with PomA. *J Biochem*. 2013; 153: 441–451. doi: [10.1093/jb/mvt011](https://doi.org/10.1093/jb/mvt011) PMID: [23420849](https://pubmed.ncbi.nlm.nih.gov/23420849/)
65. Morimoto YV, Che YS, Minamino T, Namba K. Proton-conductivity assay of plugged and unplugged MotA/B proton channel by cytoplasmic pHluorin expressed in *Salmonella*. *FEBS Lett*. 2010; 584: 1268–1272. doi: [10.1016/j.febslet.2010.02.051](https://doi.org/10.1016/j.febslet.2010.02.051) PMID: [20178785](https://pubmed.ncbi.nlm.nih.gov/20178785/)
66. Steuber J, Halang P, Vorburger T, Steffen W, Vohl G, Fritz G. Central role of the Na<sup>+</sup>-translocating NADH:quinone oxidoreductase (Na<sup>+</sup>-NQR) in sodium bioenergetics of *Vibrio cholerae*. *Biol Chem*. 2014; 395: 1389–1399. doi: [10.1515/hsz-2014-0204](https://doi.org/10.1515/hsz-2014-0204) PMID: [25205724](https://pubmed.ncbi.nlm.nih.gov/25205724/)
67. Minato Y, Fassio SR, Kirkwood JS, Halang P, Quinn MJ, Faulkner WJ, et al. Roles of the sodium-translocating NADH:quinone oxidoreductase (Na<sup>+</sup>-NQR) on *Vibrio cholerae* metabolism, motility and osmotic stress resistance. *PLoS One* 2014; 9: e97083. doi: [10.1371/journal.pone.0097083](https://doi.org/10.1371/journal.pone.0097083) PMID: [24811312](https://pubmed.ncbi.nlm.nih.gov/24811312/)
68. Zhu S, Kojima S, Homma M. Structure, gene regulation and environmental response of flagella in *Vibrio*. *Front Microbiol*. 2013; 4: 410. doi: [10.3389/fmicb.2013.00410](https://doi.org/10.3389/fmicb.2013.00410) PMID: [24400002](https://pubmed.ncbi.nlm.nih.gov/24400002/)
69. Pogoryelov D, Klyszejko AL, Krasnoselska GO, Heller EM, Leone V, Langer JD, et al. Engineering rotor ring stoichiometries in the ATP synthase. *Proc Natl Acad Sci U S A*. 2012; 109: E1599–1608. doi: [10.1073/pnas.1120027109](https://doi.org/10.1073/pnas.1120027109) PMID: [22628564](https://pubmed.ncbi.nlm.nih.gov/22628564/)
70. Gouaux E, Mackinnon R. Principles of selective ion transport in channels and pumps. *Science* 2005; 310: 1461–1465. PMID: [16322449](https://pubmed.ncbi.nlm.nih.gov/16322449/)
71. Sudo Y, Kitade Y, Furutani Y, Kojima M, Kojima S, Homma M, et al. Interaction between Na<sup>+</sup> ion and carboxylates of the PomA-PomB stator unit studied by ATR-FTIR spectroscopy. *Biochemistry* 2009; 48: 11699–11705. doi: [10.1021/bi901517n](https://doi.org/10.1021/bi901517n) PMID: [19894756](https://pubmed.ncbi.nlm.nih.gov/19894756/)
72. Terashima H, Kojima S, Homma M. Functional transfer of an essential aspartate for the ion-binding site in the stator proteins of the bacterial flagellar motor. *J Mol Biol*. 2010; 397: 689–696. doi: [10.1016/j.jmb.2010.01.050](https://doi.org/10.1016/j.jmb.2010.01.050) PMID: [20122938](https://pubmed.ncbi.nlm.nih.gov/20122938/)
73. Payandeh J, Scheuer T, Zheng N, Catterall WA. The crystal structure of a voltage-gated sodium channel. *Nature* 2011; 475: 353–358. doi: [10.1038/nature10238](https://doi.org/10.1038/nature10238) PMID: [21743477](https://pubmed.ncbi.nlm.nih.gov/21743477/)
74. Griffitt KJ, Grimes DJ. Abundance and distribution of *Vibrio cholerae*, *V. parahaemolyticus*, and *V. vulnificus* following a major freshwater intrusion into the Mississippi Sound. *Microb Ecol*. 2013; 65: 578–583. doi: [10.1007/s00248-013-0203-6](https://doi.org/10.1007/s00248-013-0203-6) PMID: [23494573](https://pubmed.ncbi.nlm.nih.gov/23494573/)